	<p align="center">PROBLEMY MECHATRONIKI UZBROJENIE, LOTNICTWO, INŻYNIERIA BEZPIECZEŃSTWA</p>
	<p align="center">PROBLEMS OF MECHATRONICS ARMAMENT, AVIATION, SAFETY ENGINEERING</p>
<p>ISSN 2081-5891; E-ISSN 2720-5266</p>	<p align="right">https://promechjournal.pl/</p>

Testing the Dynamics of Flight for the Products of Explosion for a Warhead with a Weight of 250 kg

Andrzej M. FARYŃSKI (andrzej.farynski@itwl.pl)
 Andrzej DŁUGOŁĘCKI* (andrzej.dlugolecki@itwl.pl)
 Jarosław DĘBIŃSKI (jaroslaw.debinski@itwl.pl)
 Rafał KOŃKA (rafal.konka@itwl.pl)
 Tomasz KWAŚNIAK (tomasz.kwasniak@itwl.pl)
 Łukasz SŁONKIEWICZ (lukasz.slonkiewicz@itwl.pl)
 Zbigniew ZIÓŁKOWSKI (zbigniew.ziolkowski@itwl.pl)

*Corresponding author

ORCID: <https://orcid.org/0000-0002-4357-4341>

Air Force Institute of Technology
 6 Księcia Bolesława Str., 01-494 Warsaw, Poland

*Received: July 25, 2022 / Revised: August 23, 2022 / Accepted: November 8, 2022 /
 Published: June 30, 2023.*

2023, 14 (2), 87-108; <https://doi.org/10.5604/01.3001.0053.6673>

Cite: Chicago Style

Faryński, M. Andrzej, Andrzej Długolecki, Jarosław Dębiński, Rafał Końka, Tomasz Kwaśniak, Łukasz Słonkiewicz, and Zbigniew Ziółkowski. 2023. "Testing the Dynamics of Flight for the Products of Explosion for a Warhead with a Weight of 250 kg". *Probl. Mechatronics. Armament Aviat. Saf. Eng.* 14 (2) : 87-108. <https://doi.org/10.5604/01.3001.0053.6673>



This article is an open access article distributed under terms and conditions of the Creative Commons Attribution-NonCommercial-NoDerivatives International 4.0 (CC BY-NC-ND 4.0) license (<https://creativecommons.org/licenses/by-nc-nd/4.0/>)

Abstract. This study presents the results of the testing of the explosion process of a warhead with a weight of 250 kg, filled with 87 kg of TNT with 20% of aluminium dust, in two configurations: with horizontal and vertical alignment of the warhead's longitudinal axis, and with the centre of length of the warhead body located at a height of approx. 1 m above the ground. Four warheads were detonated in each configuration. The horizontal configuration allowed the collection of some amount of the fragments from the ground, with sizes and spatial distribution of the fragments corresponding to the location on the body from which they came, with the largest fragments — from the central part of the shell — measuring approximately $9 \times 30 \times 280$ mm. For the vertical configuration, the warhead's nose was pointed downwards, with an up-down excitation. In both configurations, the explosion process was recorded from a distance of 300 m using a PHANTOM fast camera with a time resolution (frame interval) of $55 \mu\text{s}$ to $133 \mu\text{s}$: for the horizontal configuration — along the body's longitudinal axis, for the vertical configuration — perpendicular to this axis. In the vertical configuration, the body's expansion process was recorded using short-circuit sensors spaced every 5 mm along the flight radius. The sensors sent short-circuit signals to the time meter, whereas the first sensor was installed at a distance of approx. 1 mm from the body surface and was used to initiate the processes of time counting and recording the overpressure diagrams over time at the front of the explosion/shock (FU) wave. The recorded expansion velocity was approx. 1300 m/s, with the shell radius increasing by 20 mm. Overpressure at the front of the FU was measured by PCB "pencil-tip" piezoelectric sensors (CzP). Every sensor had two active surfaces arranged in "tandem" at a distance of 100 mm, which made it possible to determine the local FU velocity. Signals from CzP were recorded every 200 ns using a DEWETRON recorder with software allowing their initial and further processing. Three sensors were spaced 8 m from each other, whereas the first was located 8 m to 10 m from the warhead's longitudinal axis. Under a row of the sensors a thick-wall steel pipe was placed to protect the sensors from destruction by the fragments. The determined local FU velocities varied from approx. (590 m/s to 740 m/s) at a distance of approx. 8 m from the epicentre up to approx. 370 m/s at a distance of approx. 26 m from the epicentre; the overpressure measured values varied from approx. (230 kPa to 550 kPa) at a distance of approx. 8 m to approx. 22 kPa at a distance of approx. 26 m from the epicentre; satisfying conformance of the velocity and pressure values under the flat FU model was found. The FU trajectory was also taken from the video recording — the velocities measured varied from approx. 2,650 m/s at a distance of 0.3 m to approx. 670 m/s at a distance of 6 m from the epicentre, which corresponds to the CzP data. The fragments flying next to the CzP, generally with the highest mass to effective transverse surface ratio, left traces of their conical FU on the CzP overpressure records, which allowed the determination of average velocities for some of them across the access path to the CzP, whereas these velocities ranged from approx. 1700 m/s at a distance of approx. 8 m and (1500 m/s to 1600 m/s) at a distance of 16 m to approx. 1300 to 1400 m/s at a distance of 26 m from the epicentre. Average access velocities of the selected fragments to the field marks were determined on the basis of the video recording ranged from approx. 1800 m/s at a distance of 5 m to approx. 1500 m/s at a distance of 20 m from the explosion epicentre.

Keywords: explosion physics, fragment flight, shock wave

1. INTRODUCTION

The aim of the experiments was to master the technique of combining measurements of the properties of the fragments and shock waves (FU) generated by the heavy warheads, and obtaining the data characterising the interaction of such warheads manufactured in this country. The scope of testing included: fragment flight geometry, fragment mass and geometric characteristics, initial velocities of leading fragments, and parameters of explosion-generated airborne FU. The testing involved the use of several measurement methods, including process recording at a distance of approx. 300 m using a PHANTOM V711 fast camera with a time resolution (frame interval) from 55 μ s to 133 μ s.

The subject of the range ground testing were fragmentation and demolition warheads with a total weight $m_G = 218$ kg, maximum diameter in the central section of 273 mm, length of approx. 1500 mm, and average body thickness in the central section of 12 mm. The warhead was filled with a Tritonal explosive, which is a mixture of 80% TNT and 20% of Al dust with a weight of $m_{MW} = 87$ kg. The warhead was excited by a properly centred load of plastic explosive, initiated by an ERG electric detonator.

2. FLIGHT GEOMETRY AND FRAGMENT MASS AND GEOMETRIC CHARACTERISTICS

To determine the fragment flight geometry and the fragment weight and geometric parameters, the warheads were placed at a height of approx. 1 m above the ground on the support structure, ensuring horizontal orientation of the warhead's longitudinal axis (Fig. 1).



Fig. 1. Range test stand to study the fragment flight geometry and the fragment weight and geometric parameters — general view

To determine the fragment flight geometry, a set of 65 targets with a height of 2.5 m and a width of 1.2 m were arranged along the circumference of a semi-circle with a radius of 25 m and a vertical axis passing through the warhead's geometric centre (Fig. 1). Some of the fragments from the body bottom section — from the back of the warhead to its front section — were stopped by the ground directly below the warhead.

After sieving the soil from this area, fragments with a total weight of 43 kg were obtained, which constituted approx. 33% of the total warhead body weight (Fig. 2). For testing purposes, the fragments were divided into fine (below 5 g), medium (5–50 g) (Fig. 3), large (50–200 g) and very large (above 200 g) fragments.



Fig. 2. General view of the fragments collected during the testing



Fig. 3. Shape of typical medium fragments

Assuming process symmetry with respect to the warhead's longitudinal axis, the number of fragment holes counted on all 65 targets was converted to a sector of a sphere in a plane perpendicular to the warhead's longitudinal axis. Associating the fragment hole sizes with their weight, the quantitative and mass distribution of fragment flight was determined as a function of the declination angle between the flight direction and the warhead's longitudinal axis (zero angle corresponds to the excitation side).

The flight image data obtained using this method is presented in Fig. 4. The majority of the fragments were ejected within a 90° – 107° sector of the declination angle, with the maximum offset by 9° – 10° from the warhead's cross-section plane along with the direction of detonation wave propagation within the body.

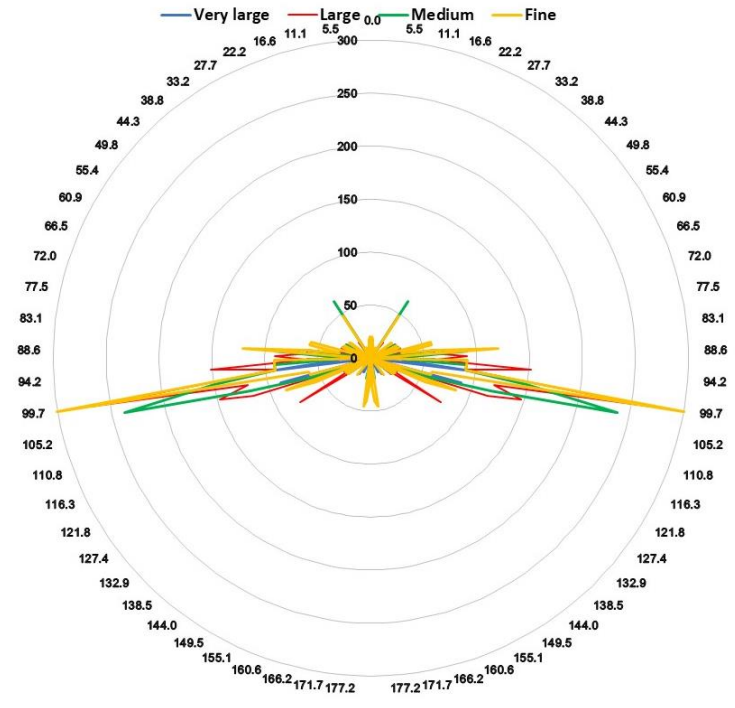


Fig. 4. Spatial distribution of the fragments with the division into four weight classes (the radial coordinate of the diagram is the number of fragments, whereas the angular coordinate is the declination of the flow of fragments)

Figure 5 presents the distribution of the number of fragments relative to the mass (m) both in the form of a histogram and approximated using a lognormal distribution (in STATISTICA — standard computer software), as follows:

$$f(m) = [1/(2\pi\sigma m)^{1/2}] \exp[-(\ln(m) - \mu)^2/2\sigma^2] \quad (1)$$

with the following parameters $\mu = 2.97$, $\sigma = 1.52$, expressed in grams, μ and σ .

Statistically half of the fragments had a weight falling within the range of approx. 8.0–52.1 g. The distribution of the fragments sizes relative to their weight is presented in Fig. 6. Averaging the sizes relative to the weight, in terms of shape a typical (average) fragment can be inscribed into a cubicoid with approximate dimensions of 49/22/8.5 mm. Very large fragments (weighing more than 200 g) came mainly from the central section — similar observations were provided by the author of [1].

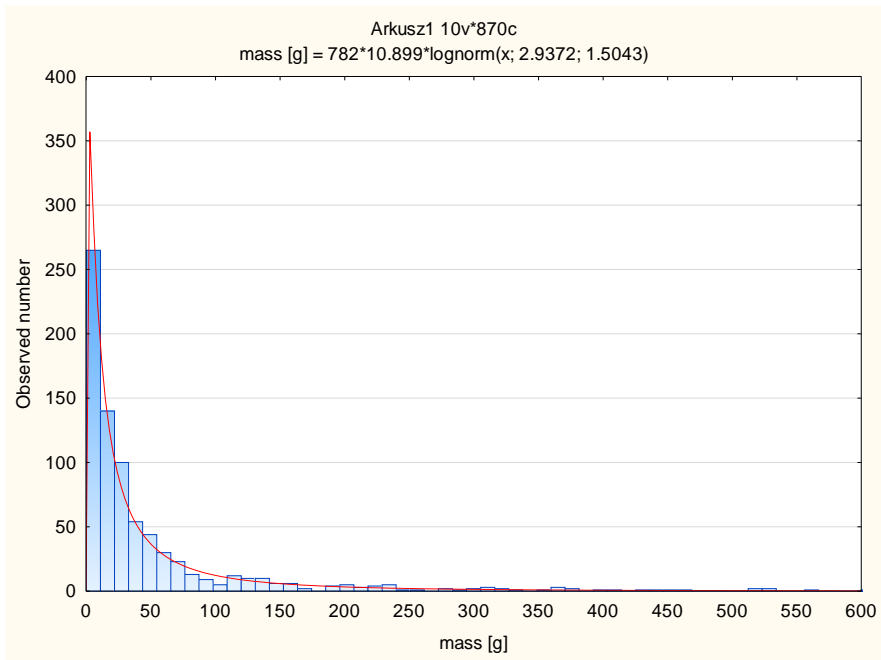


Fig. 5. Fragment weight distribution histogram (weight in grams)

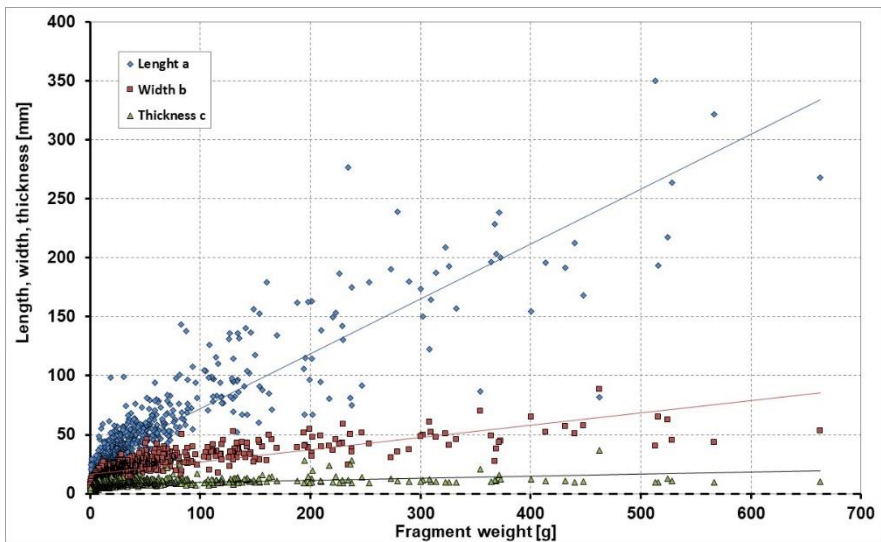


Fig. 6. Basic fragment dimensions, depending on their weight

3. MEASUREMENT OF BODY WALL EXPANSION VELOCITY

The term expansion means the initial phase of acceleration of the body wall as a continuous layer, leading to its further fragmentation. The velocity in this phase, along with the measurement of pressure values at the front of the generated FU, was measured on warheads with vertically oriented longitudinal axes, with their nose sections pointed downwards, with centres of gravity at a height of approx. 1 m above the ground, and up-down excitation.

The expansion velocity was measured using short-circuit wire sensors installed within one cross-section of the central warhead section, at the following distances: 5, 10, 15 and 20 mm, with an accuracy of ± 0.1 mm from its cylindrical surface (Fig. 7). The sensors sent a "stop" signal to corresponding channels of an MC-891 meter allowing access time measurement with an accuracy of $0.01 \mu\text{s}$. Short-circuit of the starting sensor, installed at a distance of 1 mm from the body surface, initiated the MC-891 meter. The short-circuit signal was also a reference for a DEWE3-A4 multi-channel recorder recording signals from piezoelectric pressure sensors.

Assuming immediate detonation [2] and total conversion of the chemical energy of the explosive (MW) into kinetic energy of the body and reaction products, the maximum initial velocity of the fragments (maximum expansion velocity) can be estimated using the following formula:

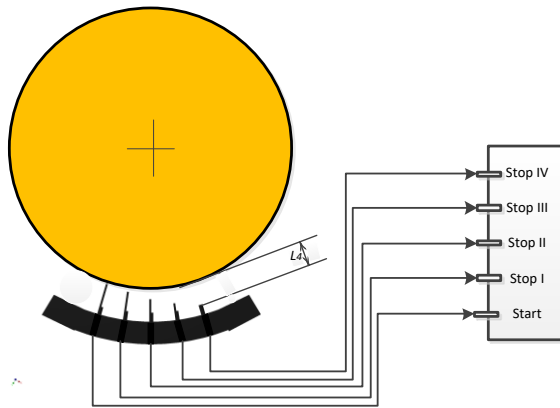
$$v_{0m} = (2U / (1/\beta + 1/2))^{1/2} \quad (2)$$

where: $\beta = m_{MW}/(m_G - m_{MW})$.

Assuming [3], [4] for TNT $U = 4$ MJ/kg, we get $v_{0m} = 1986$ m/s. However, originating from the Gurney equations with the form as above, but with the constant $(2U)^{1/2} = 2440$ m/s for TNT [5], we get $v_{0m} = 1713$ m/s or 1630 m/s for Tritonal. Using the expansion velocity equation [2]:

$$v(r) = (D/2) [\beta (1 - (r_0/r)^4)/(2 + \beta)]^{1/2} \quad (3)$$

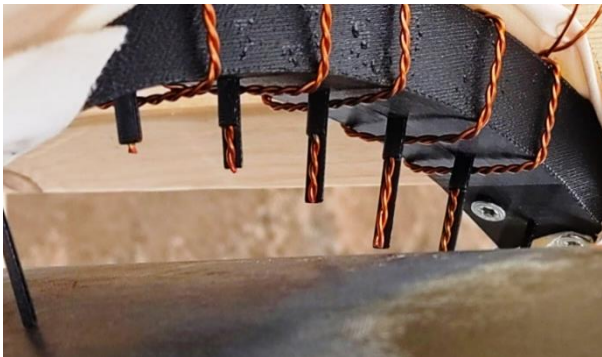
at $D = 6,860$ m/s (TNT) and $D = 6,520$ m/s for TNT/Al. 80/20 [8] and $r_0 = 137$ mm as a function of the increasing radius r of the cylindrical wall, a diagram was plotted using solid lines, as presented in Fig. 8. The same figure shows the values obtained from the measurements which were significantly lower than the theoretical ones.



(a)



(b)



(c)

Fig. 7. Short-circuit sensors to measure initial velocity of the body wall expansion phase: a) sensor wiring diagram with electronic time meter, b) and c) sensor installation on the warhead body

4. FRAGMENT VELOCITY MEASUREMENT

This measurement was carried out using 2 general methods: with flat short-circuit sensors (2 layers with Al foil with a thickness of 0.05 mm, insulated with polyethylene foil), interacting with the time meter (Fig. 9), and by performing an analysis of the frames recorded by the PHANTOM camera, where the frames, on the basis of length references placed within the explosion area, were used to track light spots assigned to specific fragments. The first method was used to obtain average velocities along the flight paths, and the second method to obtain values similar to local velocity.

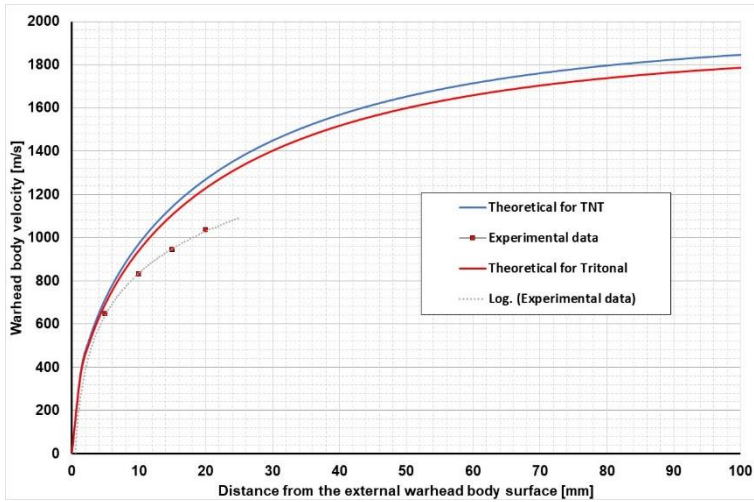


Fig. 8. Body acceleration diagram relative to theoretical diagrams



Fig. 9. Layout of flat short-circuit sensors in the field

The results of the measurements carried out using the short-circuit sensors are presented in Fig. 10, and the results of the measurements carried out by performing the frame analysis, see Fig. 11. An additional method of detecting fragment velocities was to track FU traces pulled away by the fragments flying close to these sensors on the records containing the diagrams from the pressure sensors. A fragment flying at 1500 m/s is a source of the head wave with an overpressure of approx. 2,800 kPa. The amplitude of this wave reduces along the element of the cone of the Mach wave, but it can be noticeable compared to the amplitude of the main FU generated by the explosion.

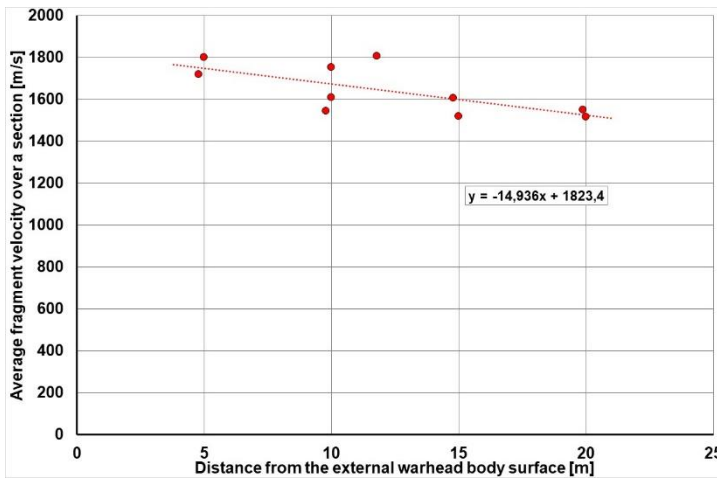


Fig. 10. Average velocities of leading fragments over the warhead – flat short-circuit sensor sections

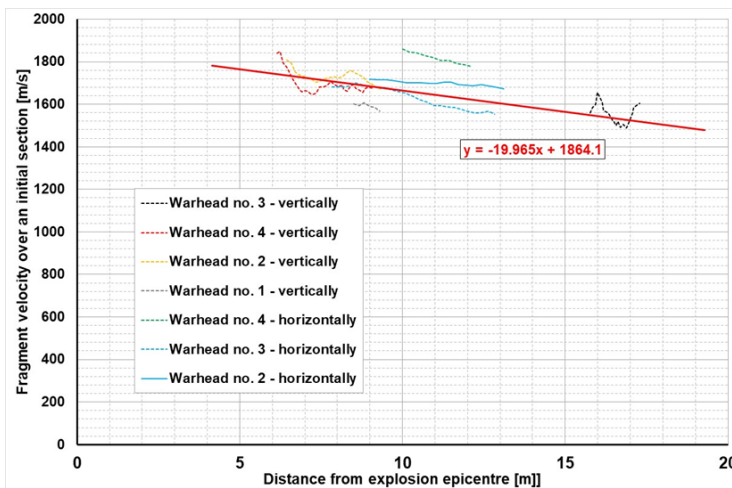


Fig. 11. Local velocity of the selected fragments determined on the basis of frame analysis from the PHANTOM camera (dotted lines illustrate the results obtained in individual trials)

Corresponding diagrams over time are described in the following section. Diagrams of FU pressure generated by flying fragments are also presented in [6].

5. EXPLOSION SHOCK WAVE DIAGNOSIS

This diagnosis included measurements of wave v_s propagation velocity and direct overpressure measurement at this wave's front Δp , whereas it can be assumed [7] that:

$$\Delta p = 2 k p_0 ((v_s / c)^2 - 1) / (k + 1) \quad (4)$$

where: p_0 — atmospheric pressure, $k = 1.4$ — air polytropic curve exponent, $c \approx 340$ m/s — speed of sound in air (depending on air temperature).

FU generation was initiated by a sphere of heated detonation products. An example image of the expansion of heated detonation products, recorded with the PHANTOM V711 camera along the warhead longitudinal axis, is presented in Fig. 12.



Fig. 12. The sequence of images presenting the expansion of a sphere of heated detonation products; the last frame shows the sphere with a radius of approx. 7 m

Diagrams of the changes in velocity of the wave front over time and the diagrams of the expansion radius determined on the basis of time-lapse analysis using the PHANTOM camera are presented in Fig. 13 and 14. Abnormally high values of velocity within the initial range of approx. 300 μ s arise from erroneous determination of the location of the observed object on the video frames. In the body expansion and fragment formation phases, the Al dust addition was an inertial component that might reduce their speed compared to the expected speed for pure TNT. In terms of energy the Al dust contributed to the explosion only after mixing the original explosion products with air, which is probably well after the fragments have left the fireball, which lasted approx. 1 s.

Afterwards the time-lapse analysis of the videos recorded using the PHANTOM camera was utilised to determine the explosion FU propagation velocity diagram over time (Fig. 15). The FU front is noticeable on the frames due to the refractive index changes on its surface.

A similar method of analysis of the FU parameters generated by anti-tank mines and mock-up explosives was used by the authors of [9].

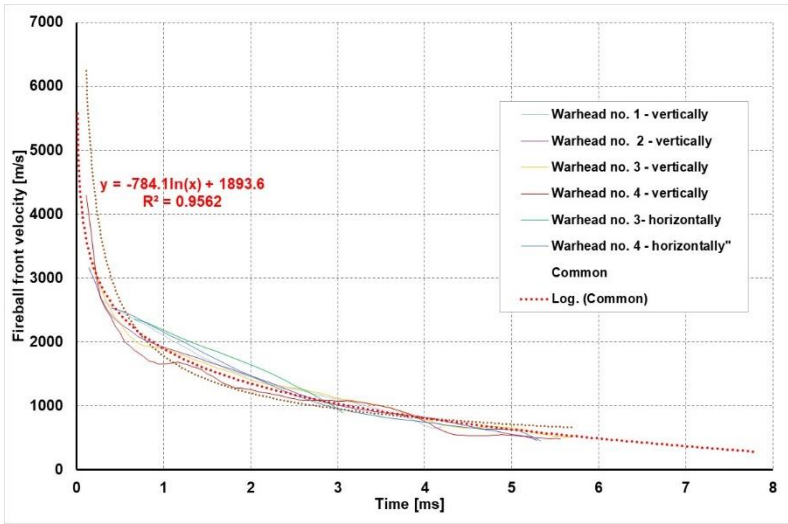


Fig. 13. Expansion velocity of the front of a sphere of heated detonation products over time obtained on the basis of PHANTOM camera frame analysis (dotted lines illustrate the results obtained in individual trials)

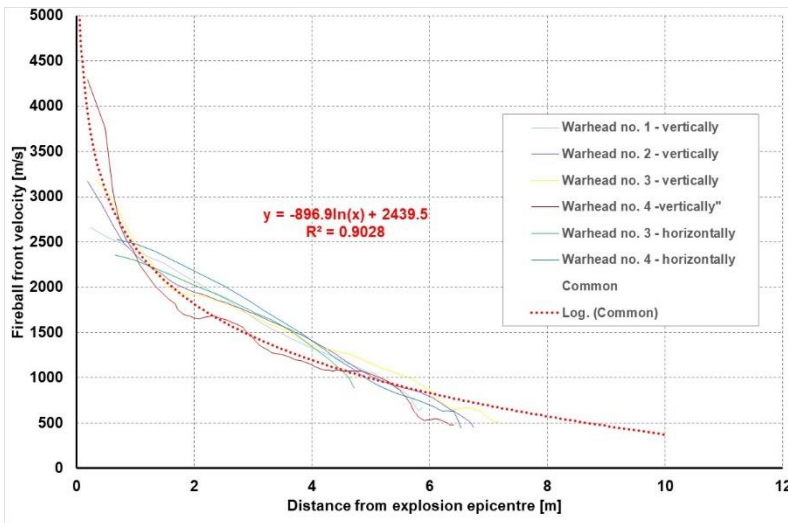


Fig. 14. The expansion velocity at the front of a sphere of heated detonation products as a function of distance from the explosion epicentre obtained on the basis of PHANTOM frame analysis (dotted lines illustrate the results obtained in individual trials)

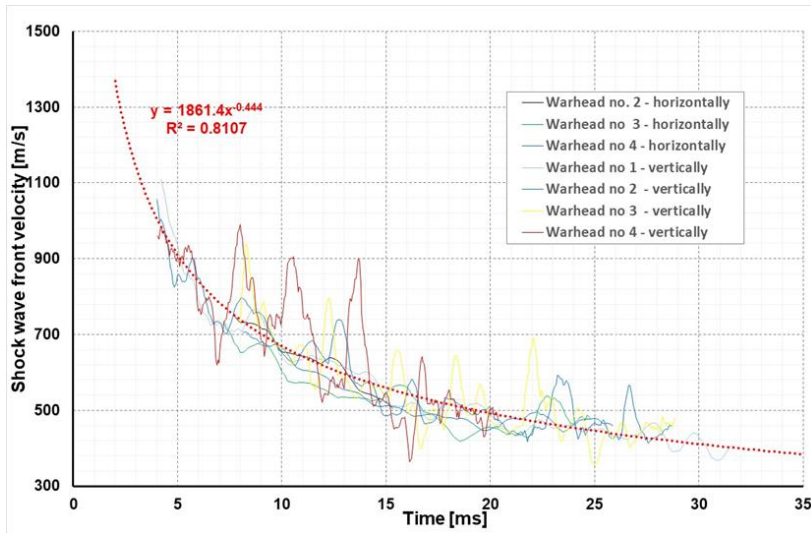


Fig. 15. FU front propagation velocity for a few fires over time obtained on the basis of the PHANTOM camera frame analysis (dotted lines illustrate the results obtained in individual trials)

Overpressure at the FU front was measured using PCB Piezotronics 137A23 pressure sensors with each sensor having two piezoelectric elements (PE) arranged in the “tandem” layout (one after the other) spaced every 100 mm, under a common deflector (Fig. 16). In the description below the first PE (according to the FU process) is marked “A”, and the second “B”. Each PE had an independent signal output to the recorder, and the rise time was approx. 2 μ s. Three such sensors were arranged along one line and spaced every 8 m relative to each other, whereas the first sensor was placed at distances 8.1 m to 10 m relative to the warhead’s vertically oriented longitudinal axis. To protect from the damaging effects of the fragments, 2 thick-walled steel pipes with an external diameter of 80 mm were placed at a distance of 2 m in front of the first sensor, one after another, as in [6]. Signals from the sensors were stored in the DEWETRON DEWE3-A4 multi-channel recorder, every 200 ns. The record initial point ($t = 0$) was determined by the position of the pulse sent at the short circuiting of the starting sensor by the expanding body. The recorder’s software allowed further processing of its records.



Fig. 16. Top: PCB 137A23 dual pressure sensor — general view. Bottom: method of arrangement of the pressure sensors relative to the warhead. The pipe protection for the sensors can be seen on the left

Figure 17 shows an example of an overpressure diagram at the explosion FU front, passing successively through all “A” sensors. The proper overpressure increase at the front was preceded by disturbances which were particularly intensive at a distance of more than a dozen metres from the epicentre. The disturbances were initiated by the “leading” body fragments, followed by a hard-to-identify mixture of sand, secondary stone fragments, as well as ricocheting fragments excited by the explosion. The “leading” body fragments (Fig. 18) recorded characteristic profiles corresponding to their conical shock waves. The times of occurrence of each profile of the first fragments flying by at the subsequent waves near consecutive pressure sensors allowed the diagram (Fig. 19) to be plotted to additionally present the rate of change of the velocities of the fastest fragments along their flight trajectories. The character of the velocity rates of change and numerical values on this diagram are very similar to the ones presented in Fig. 10 and 11.

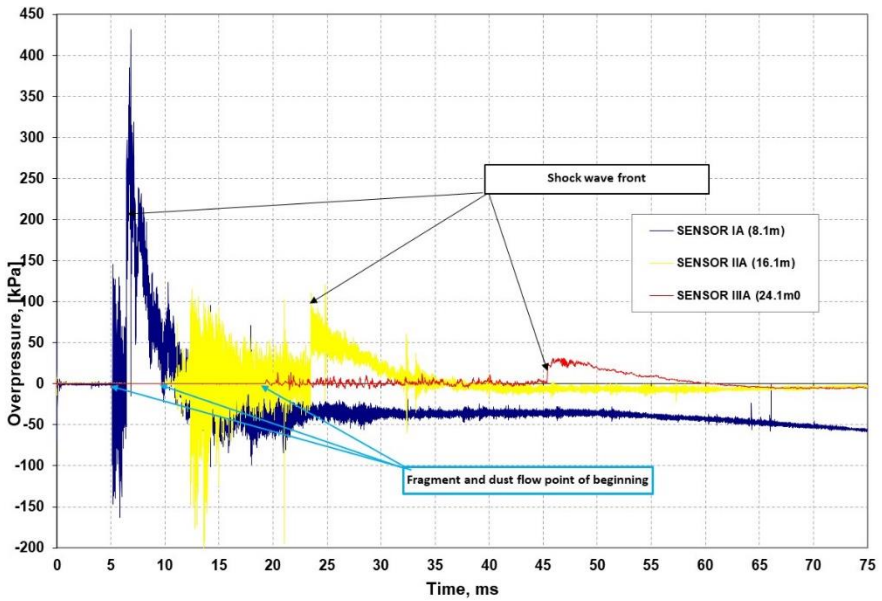


Fig. 17. An example of continuous storage of signals received from the pressure sensors on the DEWE3-A4

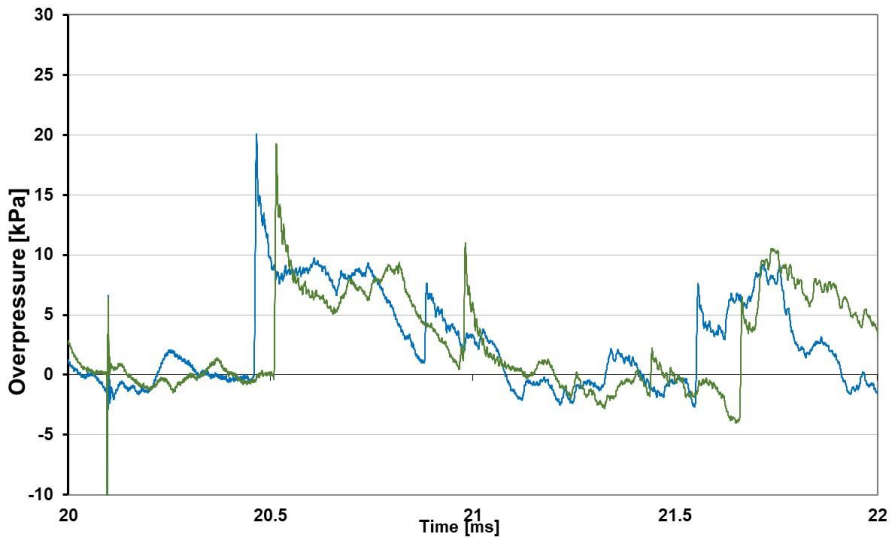


Fig. 18. A fragment of the recorded diagram with visible disturbance caused by shock waves generated by flying fragments

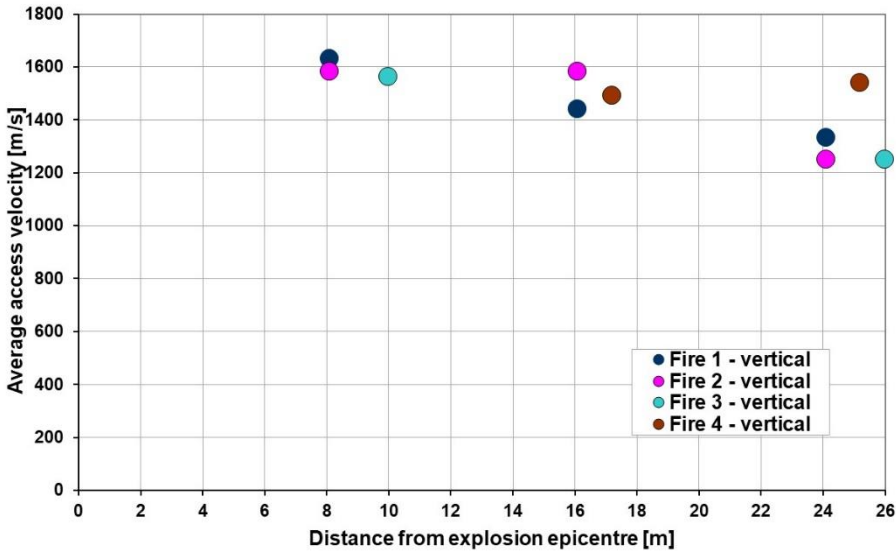


Fig. 19. Average velocity of leading fragments over distances measured from the warhead to the sensors

Figure 20 shows an example diagram with overpressure pulses at the FU front recorded by PE “A” and “B” of the same sensor. FU access to PE “A” and “B” time differences in subsequent sensors were used to determine the local wave velocities v_s used to calculate, according to the formula (4), the values of overpressure Δp measured simultaneously by the sensors at the measuring points. The common scope of the determined diagrams of v_s and calculated Δp as a function of distances from explosion epicentres is presented in Fig. 21. Figure 22 shows the calculated and measured values of overpressure for one of the fires as a function of distance from the explosion epicentre. Note that for a given sensor position, generally two different overpressure values are marked that correspond to the measurements of, respectively, PE “A” and “B” and one value resulting from velocity measurement. This results from the fact that, despite the FU access times to the measuring point being properly specified by the FU front increase time lasting a few microseconds, the explosion FU amplitudes at “A” and “B” result from its interference with fragment FU, diffraction at the sensor body and other disturbances.

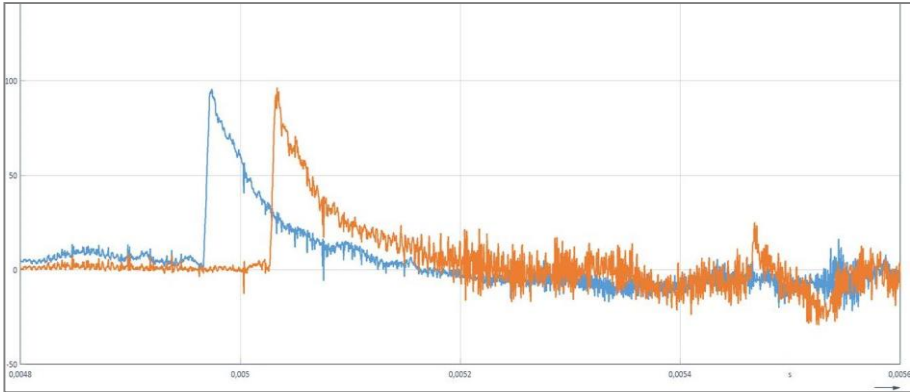


Fig. 20. An example overpressure diagram over time at the FU front recorded by “A” and “B” measuring elements of the dual pressure sensor [abscissa — time (s), ordinate — overpressure (MPa)]

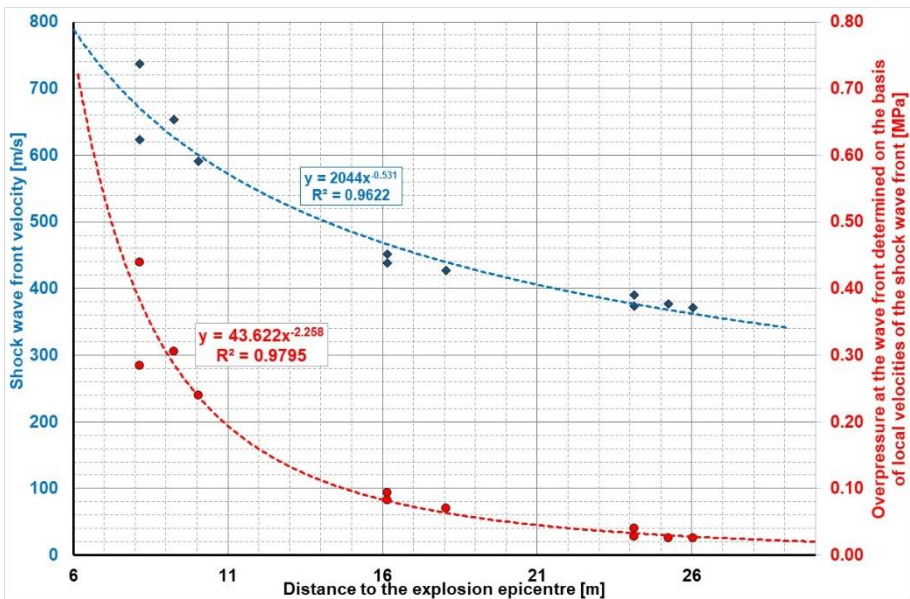


Fig. 21. Local FU front propagation velocity over time from the explosion epicentre determined on the basis of the time of wave front penetration through “A” and “B” elements of the piezoelectric sensors and overpressure at the wave front specified according to formula (4)

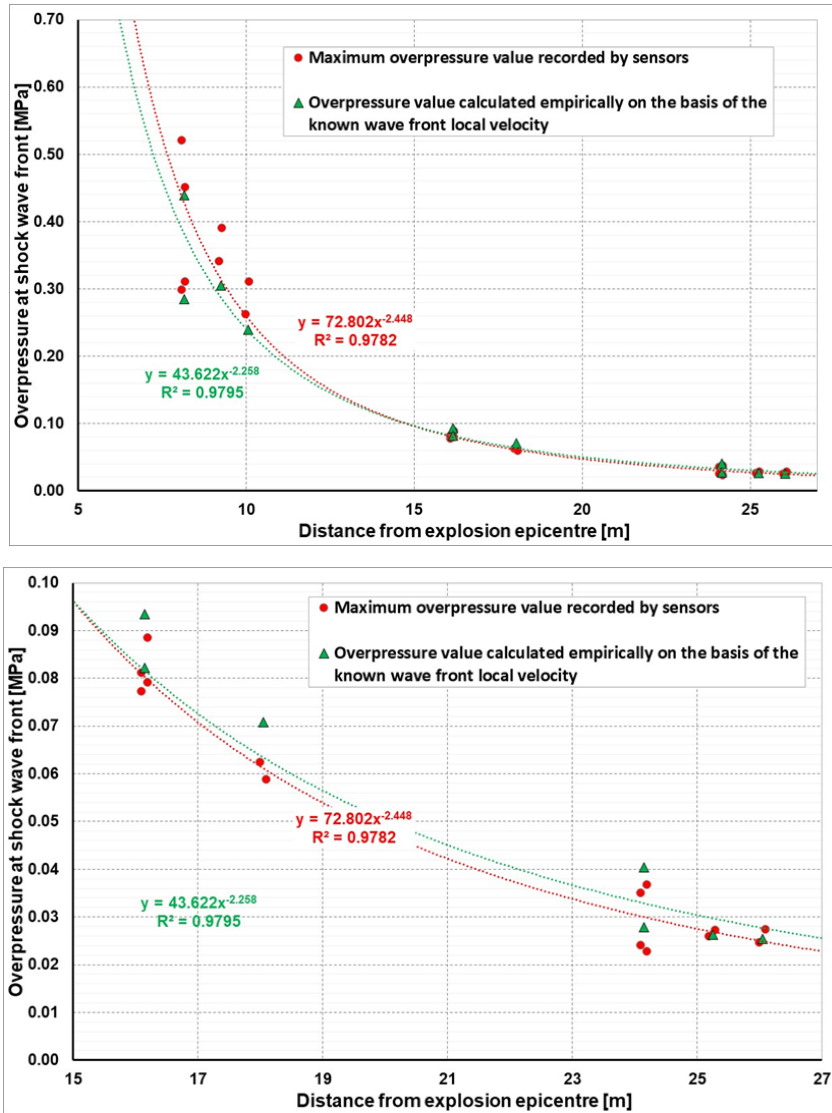


Fig. 22. Comparison of calculated and directly measured overpressure values at the FU front; upper diagram — full scope, lower diagram — zoomed in fragment of low pressure area

6. CONCLUSIONS

- The measured velocity of the warhead wall expansion at the initial explosion phase occurred approx. 1100 m/s after the warhead radius increase by 20 mm and was significantly lower than theoretical estimates.
- The weight of half the steel fragments was approx. 8–52 g. A weight averaged fragment could be inscribed as a cubocoid with approximate dimensions of 49/22/8.5 mm. The lowest dimension corresponds to the thickness of the body cylindrical wall at cracking, which means that the fragmentation occurred upon a warhead diameter increase by approx. 40%.
- The majority of the fragments was ejected within a sector 90° – 107° of the declination angle, with the maximum offset by 9° – 10° from the warhead's cross-section plane along with the direction of detonation wave propagation within the body.
- The velocities of “leading” fragments were approx. 1700 m/s at a distance of 5 m and approx. 1400 m/s at a distance of 25 m from the explosion epicentre.
- The local FU velocities varied from approx. 590–740 m/s at a distance of approx. 8 m to approx. 370 m/s at a distance of approx. 26 m from the epicentre.
- Overpressure values at the explosion FU front varied from approx. 230–550 kPa at a distance of 8–10 m from the epicentre at the positive part of the pulse $\tau_+ \approx 6.7$ ms - to approx. 22–27 kPa at a distance of 25 m from the epicentre at $\tau_+ \approx 16$ ms.
- The method of protection of the pressure sensors from the fragments in the form of a thick-wall pipe protecting the angular sector 0.5 – 0.7° efficiently secures the sensors against irreparable damage.
- The profiles of the shock waves of the fragments flying near the pressure sensors noticeable on the overpressure diagrams allowed for additional diagnosis of fragment velocity; overpressure amplitudes corresponding to these profiles were approx. 20–90 kPa, meaning they were comparable to the explosion FU overpressures.
- The DEWE3-A4 multi-channel recorder considerably facilitated the analysis of the obtained results; in connection with the tandem piezoelectric sensors, it enabled the synchronous recording of the common time axis of the phenomena occurring during the warhead explosion.

FUNDING

The authors received no financial support for the research, authorship, and/or publication of this article.

REFERENCES

- [1] Starczewski, Lech. 2017. Badanie fragmentacji naturalnej nowej drobnoziarnistej stali na kadłuby pocisków odłamkowych. W *Materiały VI Konferencji Naukowo-Technicznej*, Kołobrzeg.
- [2] Stanyukovich, K.P. et al. 1975. *Physics of Explosion* (in Russian). Moscow: Nauka.
- [3] Knoepfel, Heintz. 1970. *Pulsed High Magnetic Fields: Physical Effects and Generation Methods Concerning Pulsed Fields Up to the Megaoersted Level*. Amsterdam, London: North-Holland Publishing Company.
- [4] <https://pl.wikipedia.org>
- [5] Flis, J. William. 1996. Gurney formulas for explosive charges surrounding rigid cores. In *Proceedings of the 16th International Symposium on Ballistics*, San Francisco, CA, 23-27 September 1996. Dyna East Corporation, 3620 Horizon Drive, King of Prussia, Pa., U.S.A
- [6] Długolecki, Andrzej, Jarosław Dębiński, Andrzej Faryński, Tomasz Kwaśniak, Łukasz Słonkiewicz, and Zbigniew Ziółkowski, 2021. "Measurements of characteristics for fragmentation – bursting heads". *Problemy Techniki Uzbrojenia* 157 (2) : 59-79.
- [7] Rościszewski, Jan. 1957. *Aerodynamika stosowana*. Warszawa: Wydawnictwo MON.
- [8] Cudziło, Stanisław, and Waldemar A. Trzcński. 2014. "Melt Cast High Explosives" (in Polish). *Biuletyn WAT* LXIII (4) : 43-55.
- [9] Saska, Piotr, Edyta Krzystała, and Jerzy Czmochoński. 2011. "Analysis of shock wave parameters determined empirically with the use of a high-speed camera" (in Polish). *Modelowanie Inżynierskie* 11 (42) : 385-393.

Badanie dynamiki rozlotu produktów wybuchu głowicy o wagomiarze 250 kg

Andrzej DŁUGOŁĘCKI, Jarosław DEBIŃSKI, Andrzej FARYŃSKI,
Rafał KOŃKA, Tomasz KWAŚNIAK, Łukasz SŁONKIEWICZ,
Zbigniew ZIÓŁKOWSKI

*Instytut Techniczny Wojsk Lotniczych
ul. Księcia Bolesława 6, 01-494 Warszawa*

Streszczenie. W ramach prezentowanej pracy przedstawiono wyniki badań procesu wybuchu głowicy o wagomiarze 250 kg, wypełnionej 87 kg TNT z domieszką 20% pyłu Al., w dwu konfiguracjach: o poziomym i pionowym umiejscowieniu osi podłużnej głowicy, przy czym w obu wypadkach środek długości korpusu głowicy znajdował się ok. 1 m nad powierzchnią gruntu. W każdej konfiguracji zdetonowano po 4 egzemplarze. Konfiguracja pozioma pozwoliła na zebranie z gruntu pewnej ilości odłamków o rozmiarach i rozkładzie przestrzennym odpowiadającym miejscu w korpusie, z którego zostały wyrwane – największe – ze środkowej części skorupy – miały przybliżone wymiary $9 \times 30 \times 280$ mm. Przy konfiguracji pionowej nos głowicy zwrócony był w dół i pobudzenie następowało od góry. W obu konfiguracjach proces wybuchu filmowano z odległości 300 m przy pomocy szybkiej kamery PHANTOM o wykorzystywanej rozdzielczości czasowej (interwał między kadrami) 55 mikrosekund do 133 mikrosekund: przy poziomej – wzdłuż osi podłużnej korpusu, przy pionowej – prostopadle do niej. W konfiguracji pionowej proces rozpękania korpusu był rejestrowany za pomocą czujników zwarciovych rozmieszczonych co 5 mm wzdłuż promienia rozlotu, podających sygnał zwarcia na licznik czasu, przy czym pierwszy czujnik znajdował się w odległości ok. 1 mm od powierzchni korpusu i służył do inicjowania procesów: zliczania czasu oraz rejestracji przebiegów czasowych naciśnienia na froncie fali podmuchowej/ uderzeniowej (FU) wybuchu. Zmierzona prędkość rozpękania wynosiła ok. 1300 m/s po zwiększeniu promienia skorupy o 20 mm. Naciśnienie na froncie FU mierzone było za pomocą „ołówkowych” piezoelektrycznych czujników (CzP) firmy PCB, z których każdy zawierał dwie powierzchnie czynne rozmieszczone w układzie „tandem” w odległości 100 mm, co pozwalało na wyznaczenie lokalnej prędkości FU. Sygnały z CzP były zapisywane z krokiem 200 nanosekund na rejestratorze firmy DEWETRON, wyposażonym w oprogramowanie pozwalające na wstępną i dalszą ich obróbkę. Trzy czujniki ustawiano w odległości 8 m od siebie, przy czym pierwszy w odległości 8 m do 10 m od osi podłużnej głowicy. Przed rzędem czujników stawiano grubościenną rurę stalową zabezpieczającą je przed zniszczeniem przez odłamki. Wyznaczone lokalne prędkości FU zmieniały się od ok. (590 m/s do 740 m/s) w odległości ok. 8 m od epicentrum - do ok. 370 m/s w odległości ok. 26 m od epicentrum; zmierzone przy tym wartości naciśnienia zmieniały się od ok. (230 kPa do 550 kPa) w odległości ok. 8 m, do ok. 22 kPa w odległości ok. 26 m od epicentrum; stwierdzono zadowalającą zgodność prędkości i ciśnień w ramach modelu płaskiej FU.

Trajektorię FU odczytywano również z zapisu filmowego – zmierzone tak prędkości zmieniały się od ok. 2650 m/s w odległości 0.3 m do ok. 670 m/s w odległości 6 m od epicentrum, co dobrze się zgadza z danymi z CzP. Przelatujące obok CzP odłamki, na ogół o największym stosunku masy do efektywnej powierzchni poprzecznej, zostawiały na zapisach nadciśnień z CzP ślady swoich stożkowych FU, co pozwalało na wyznaczenie dla niektórych z nich prędkości średnich na trasie dolotu do CzP, które zmieniały się od ok. 1700 m/s w odległości ok. 8 m i (1500 m/s do 1600 m/s) w odległości 16 m do ok. (1300÷1400 m/s) w odległości 26 m od epicentrum. Wyznaczone z zapisu filmowego średnie prędkości dolotu wybranych odłamków do znaczników terenowych zmieniały się od ok. 1800 m/s w odległości 5 m do ok. 1500 m/s w odległości 20 m od epicentrum wybuchu.

Słowa kluczowe: fizyka eksplozji, lot odłamków, fala uderzeniowa